Scientific article
UDC 54-386:546.654:547.831.7
DOI: 10.52957/2782-1900-2026-7-1-114-124

LANTHANUM(III) COMPLEX WITH 8-OXYQUINOLINE: SYNTHESIS, SPECTRAL PROPERTIES, AND BIOLOGICAL ACTIVITY PROFILE

A.A. Shubina, T.N. Orlova

Anna Alexandrovna Shubina, Student**; Tatyana Nikolaevna Orlova,** Candidate of Chemical Sciences, Associate Professor
P.G. Demidov Yaroslavl State University, Sovetskaya St., 14, Yaroslavl, Russia, 150003;
annashubina100@gmail.com, eagle0802@mail.ru.

Keywords:
8-oxyquinoline, IR spectroscopy, electron spectroscopy, lanthanum, complex formation, coordination number, complex stability, PASS-online.

Abstract. *The research examines the coordination of lanthanum(III) compound with 8-oxyquinoline. The article analyses the synthesis method resulted in the formation of a yellow fine-crystalline precipitate. The structure and nature of ligand coordination with the metal ion were confirmed by physicochemical methods (electron and vibrational spectroscopy) and semi-empirical quantum chemical calculations (MOPAC//PM7). Electronic spectroscopy records a significant bathochromic shift (Δλ=72 nm). It indicates the formation of a stable complex. The research reveals the dependence of the complex stability on the pH of the medium, and identifies the its optimal pH range of 7.0–8.0. The theoretical part of the research includes quantum chemical modeling to evaluate the redistribution of electron density, and visualise the optimised geometry of the molecule. Moreover, computer analysis of biological activity and pharmacokinetic parameters (ADME-Tox) indicates the potential value of the synthesized complex as a compound with a modified and improved biological activity profile.*

For citation:
Shubina A.A., Orlova T.N. Lanthanum(III) complex with 8-oxyquinoline: synthesis, spectral properties, and biological activity profile // From Chemistry towards Technology Step-by-Step. 2026. Vol. 7, Iss. 1. P. 114-124. URL: https://chemintech.ru/ru/nauka/issue/7073/view

Introduction

8-hydroxyquinoline (8-quinolinol) is an asymmetric six-membered ring ligand [1]. It is one of the most well-known universal chelating agents [2] in analytical practice [3], photonics, and photophysics [4]. By coordinating with metal ions (Cu^{2+}, Be^{2+}, Mg^{2+}, Bi^{3+}, Ni^{2+} etc.) through the oxygen of the hydroxyl group and the nitrogen of the quinoline ring [5], it forms very stable complex compounds [6] (see Scheme 1). Their logarithms of stability constants (depending on pH and solvent used) could reach lg β ≈ 20-22 [7]. Moreover, the presence of a phenolic group gives 8-oxyquinoline high reactivity in electrophilic aromatic substitution [8], diazotization, and the ability to participate in rearrangements [9].

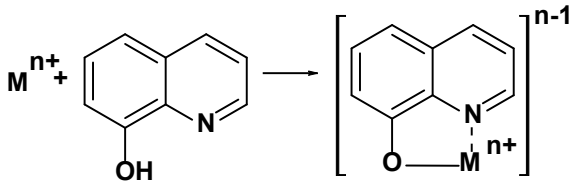

Scheme 1. Complex formation of 8-oxyquinoline with metals.

Its high chelating ability has attracted the interest of researchers (beginning in the 20th century) in studying the biological properties of this ligand and its complexes [10]. Its antifungal and antibacterial properties have been studied most extensively [11]. This ability is explained by the binding of metal ions as cofactors of microbial enzymes into a stable complex [12]. Thus, 8-oxyquinoline and its derivatives are widely used in medicine as local antiseptics [13], as well as in agriculture for plant protection [14].

Nowadays, scientists consider 8-oxyquinoline and its complexes to be promising anti-cancer drugs and agents against human immunodeficiency virus, leishmaniasis, and schistosomiasis [15]. Although researchers from different countries have experimentally observed the antibacterial and cytotoxic activity of transition element complexes with 8-oxyquinoline and its derivatives [16-19]. However, the issue of compound interaction with a specific biological target has not yet been sufficiently studied.

Purpose of the paper

The purpose of this study is to synthesise, investigate the spectral and analytical characteristics, and profile the possible biological activity of the La(III) complex with 8-oxyquinoline.

Experimental part

To synthesise the compound under study, we used the following reagents: isopropyl alcohol, chemically pure 99.8% (EKOS-1 AO, Russia), 8-oxyquinoline, chemically pure (LenReaktiv AO, Russia), lanthanum nitrate hexahydrate, chemically pure (LenReaktiv AO, Russia).

Method for synthesising a La(III) complex with 8-oxyquinoline. 0.43 g of lanthanum (III) nitrate was dissolved in 5 ml of distilled water with constant magnetic stirring. We added 0.14 g of 8-hydroxyquinoline, previously dissolved in 5 ml of isopropyl alcohol to the resulting solution. After 2-3 minutes, a yellow fine crystalline precipitate was observed; it was filtered and washed with distilled water and isopropyl alcohol, then dried in an oven for 2 hours at 60°C. The product weight is 0.19 g; the yield is 68%. The resulting compound is easily soluble in DMSO, DMFA, and acetonitrile, moderately soluble in chloroform, and very slightly soluble in distilled water, and 96% ethanol [20].

Main body

Electronic spectra were recorded using a PE 5400-UV spectrophotometer (EKROSHIM OOO, Russia); infrared spectra were recorded using a Spectrum 65 device (Perkin Elmer).

Interpretation of the IR spectrum data (see Figs. 1, 2) showed that the compound obtained did not have a peak at 3047 cm^{-1} corresponding to the hydroxyl group. This confirms its participation in coordination. The spectra of the ligand and complex also contain key bands of the quinoline nucleus at 1620-1940 cm^{-1} for valence vibrations C=N, C=C, as well as out-of-plane aromatic vibrations C-H in the range 900-650 cm^{-1}. Table 1 presents a more detailed comparative analysis.

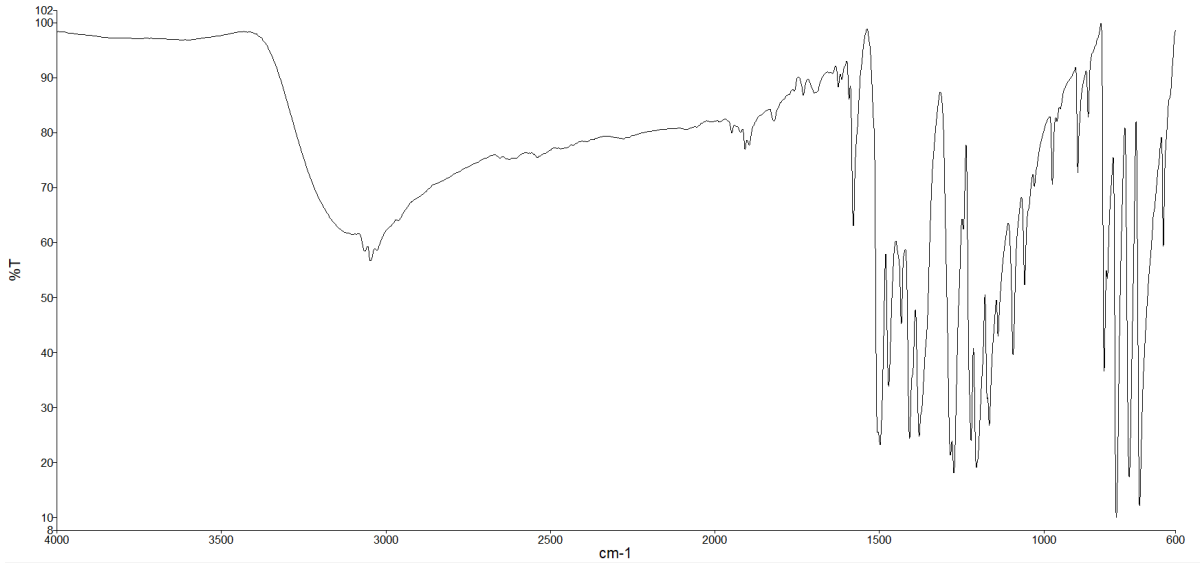

Fig. 1. IR spectrum of 8-oxyquinoline (ligand)

Fig. 2. IR spectrum of La(III) complex with 8-oxyquinoline

Table 1. Wavelengths in the IR spectrum of 8-oxyquinoline and the La(III) complex with 8-oxyquinoline

Vibration mode	Ligand wave numbers, cm^{-1}	Complex wave numbers, cm^{-1}	Interpretation
ν(C-O), phenolic	1244.9 (high intensity)	1233.8	coordination via –OH with deprotonation
C=N, ν(C=C)	1624.8	1600.5	participation of the heterocyclic N quinoline nucleus in coordination; redistribution of electron density
neighboring aromatic modes	1592.3; 1579.2	1600.5; 1569.0	redistribution of charges in the quinoline nucleus during complex formation
O-H	3047.1 (medium intensity)	complete disappearance	coordination via –OH
fingerprint area, La^{3+}-O, La^{3+}-N	636.9	657.0	indicator of metal–ligand bonding

Additionally, the structural changes occurred when La^{3+} was added to the solution are confirmed by the electronic spectrum (see Fig. 3): a bathochromic shift from λ_{max1}=307 nm to λ_{max2}=379 nm is observed during complex formation. Thus, the formation of coordination bonds reduces the energy gap between the HOMO (highest occupied molecular orbital) and the LOMO (lowest unoccupied molecular orbital). It is accompanied by the appearance of charge transfer bands.

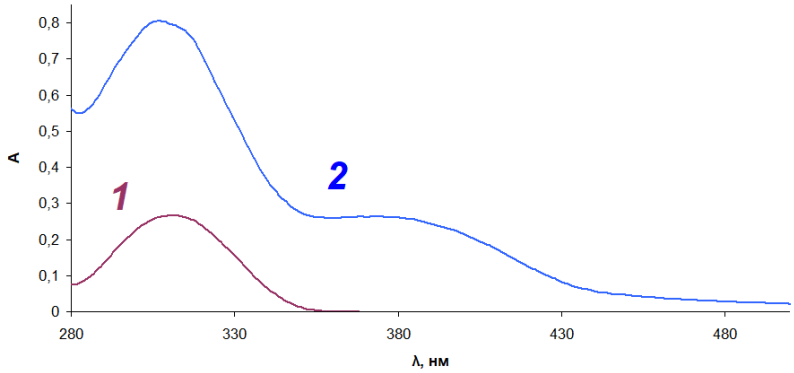

Fig. 3. Electronic spectrum of 8-oxyquinoline (curve 1) and the complex compound La(III) with 8-oxyquinoline (curve 2).

The coordination number of the lanthanum (III) complex with 8-oxyquinoline was determined using the molar ratio method. The dependence of the optical density of the solution at λ_{max}=379 nm on the ligand concentration (C_L) at a constant complexing agent concentration (C_K) was studied - see Table 2.

Table 2. Absorption of complexing agent (La^{3+}) and 8-oxyquinoline ligand solutions by saturation method

Measurement No.	V of La^{3+} solution C=0.01 M, ml	V of 8-oxyquinoline solution C = 0.05 M, ml	n(La^{3+}):n(8-oxyquinoline), mole	V(H_2O), ml	V_{total}, ml	A
1	1	0.2	1:1	0.8	2	0.432
2	1	0.4	1:2	0.6	2	0.836
3	1	0.6	1:3	0.4	2	1.108
4	1	0.8	1:4	0.2	2	1.159
5	1	1	1:5	0	2	1.161

The equivalence point on the graph showing the dependence of solution absorption on the ratio of ligand to complexing agent (see Fig. 4) is equal to 3. Thus, the complex is formed in a ratio of 1:3.

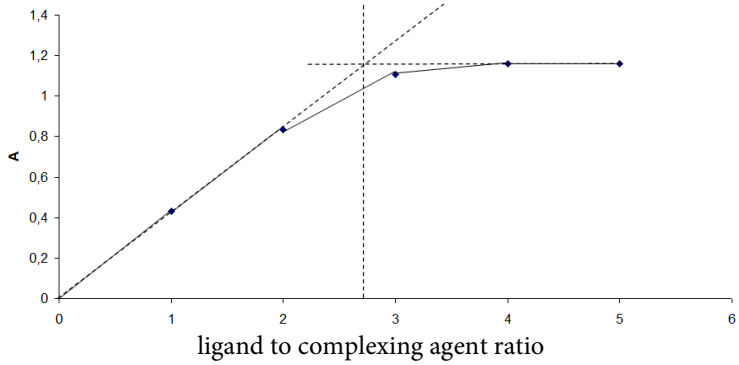

Fig. 4. Graph showing the dependence of absorption of solutions containing ligand and complexing agent $n(La^{3+})$:n(8-oxyquinoline)

The spectrophotometric method was used to determine the stability range of the coordination compound at different pH values. A series of solutions of the 8-oxyquinoline complex with a constant concentration of the test substance ($C=2.1\cdot10^{-5}$ M) was prepared; double-distilled water was used as the solvent. Buffer solutions with the required pH values in the range of 3.0-10.0 were prepared based on individual buffer systems (acetate for 3.0-5.0, ammonia for 9.0-10.0). In the neutral range (pH 7.0–8.0), the use of commonly available buffer systems was limited due to their unsuitability: acetate buffer (pK_a = 4.76) does not have sufficient buffer capacity at pH > 6; ammonia buffer (pK_a = 9.25) does not have sufficient buffer capacity at pH < 8.5 [21]. In the pH range of 6.5–8.5, the pH value was maintained by directly adding small amounts of diluted HCl or NaOH solutions (C = 0.1 M) to the test solution containing the background electrolyte (KNO_3, C = 0.1 M). Control of pH was performed using a potentiometric method. The resulting solution was thermostated at a temperature of 25.0±0.1 ^{0}C for 30 minutes to establish equilibrium; then the optical density values were determined.

We measured the absorption at λ_{max}=379 nm for each of the solutions. Their decrease relative to the maximum indicates low stability of the complex at this pH value. Table 3 summarises the experimental data.

Table 3. Absorption of complexing agent (La^{3+}) and 8-oxyquinoline ligand solutions by saturation method

Sample No.	pH	Buffer system	System buffer range	A
1	3.0	Acetate	3.6-5.6	0.217
2	4.0	Acetate	3.6-5.6	0.351
3	5.0	Acetate	3.6-5.6	0.396
4	6.0	Acetate	3.6-5.6	0.547
5	7.0	pH adjusted with HCl or NaOH	-	0.671
6	8.0	pH adjusted with HCl or NaOH	-	0.699
7	9.0	Ammonia	8.2-10.2	0.526
8	10.0	Ammonia	8.2-10.2	0.422

The graph showing the dependence of absorption on pH for the lanthanum complex with 8-oxyquinoline has a bell-shaped curve (see Fig. 5).

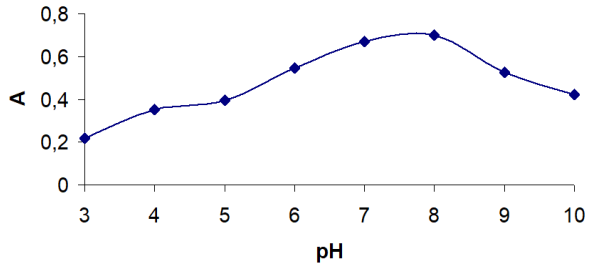

Fig. 5. Graph showing the dependence of the pH of a solution containing a La(III) complex with 8-oxyquinoline on the absorption value at λ_{max}=379 nm

In an acidic environment, the concentration of H^+ ions is high; the ligand is protonated. This is a process that competes with complex formation:

$$[La(C_9H_6NO)_3] + 3H^+ \rightarrow La^{3+} + 3C_9H_7NO^+$$

In an alkaline environment, starting at pH=8, there is a tendency for La^{3+} ions to hydrolyse and form first finely dispersed and then larger agglomerates of lanthanum (III) hydroxide. It also disrupts the integrity of the coordination compound:

$$[La(C_9H_6NO)_3] + 3OH^- \rightarrow La(OH)_3\downarrow + 3C_9H_6NO^-$$

Studying the dependence of lanthanum(III) complex stability with 8-hydroxyquinoline on the pH of the medium is important in terms of the prospects for biomedical application of this compound [22]. Thus, it is possible to forecast the stability and probability of complex destruction. It leads to the release of La^{3+} ions and ligands ensuring targeted drug delivery [23].

We obtain the theoretical data on complex formation. Geometry optimisation was performed (see Figs. 6 and 7), quantum chemical calculation of charges, and the energy gap between HOMO and LOMO using the semi-empirical RM7 method in the MOPAC program [24]. Structures were visualised using ChemCraft v. 1.6. [25].

$$\Delta E_{ligand}=|E_{HOMO}-E_{LOMO}|=|36.0628-30.8269|=5.2359 \text{ eV}$$

$$\Delta E_{complex}=|E_{HOMO}-E_{LOMO}|=|36.0310-32.3806|=3.6504 \text{ eV}$$

$$\Delta E_{total}= \Delta E_{ligand}- \Delta E_{complex}=1.5855 \text{ eV}$$

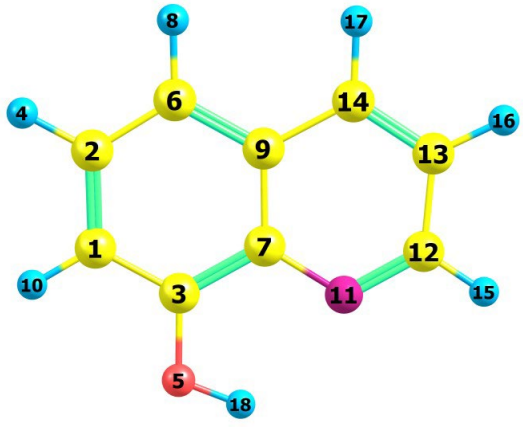

Fig. 6. Optimised geometry of the 8-oxyquinoline molecule: $l_{average}$ (C-H)=1.09 Å, $l_{average}$ (C-C)=1.41 Å, l(O-H)=1.00 Å, l(C-N)=1.37 Å, ∠(H-O-C)=40.3°.

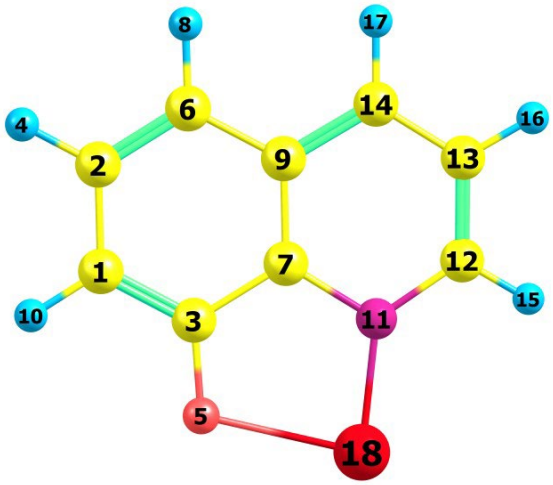

Fig. 7. Optimised geometry of the La(III) complex with 8-oxyquinoline: $l_{average}$ (C-H)=1.08 Å, $l_{average}$ (C-C)=1.38 Å, $l(La^{3+}\text{-}O)$=2.27 Å, $l(La^{3+}\text{-}N)$=1.86 Å, l(C-N)=1.41 Å, ∠(O-La-N)=81.2°.

A study of the charges on 8-oxyquinoline and its lanthanum derivative atoms showed a redistribution of electron density. It is also confirmed by a comparison of C-C bond lengths (their decrease in the case of coordination bonding with the metal) and coordination not only through the hydroxyl group, but also through the nitrogen of the quinoline ring (see Table 4): a more negative charge is observed on nitrogen (Δq_N=0.453; Δq_O=0.426), and a positive charge on lanthanum (q_{La}=+1.359). Deprotonation of the ligand forms a stable chelate compound.

Table 4. Charges on 8-hydroxyquinoline and La(III) complex with 8-hydroxyquinoline

	Ligand		Complex	
Atom number	Atom type	Charge	Atom type	Charge
1	C	-0.271	C	-0.300
2	C	-0.068	C	-0.077
3	C	+0.292	C	+0.393
4	H	+0.156	H	+0.150
5	O	-0.448	O	-0.874
6	C	-0.226	C	-0.252
7	C	+0.012	C	+0.010
8	H	+0.161	H	+0.158
9	C	-0.013	C	+0.040
10	H	+0.182	H	+0.175
11	N	-0.373	N	-0.826
12	C	+0.054	C	-0.042
13	C	-0.218	C	-0.144
14	C	-0.103	C	-0.197
15	H	+0.174	H	+0.119
16	H	+0.167	H	+0.153
17	H	+0.163	H	+0.157
18	H	+0.358	La	+1.359

Analysis of possible biological activity profile in the PASS Online program [26] for 8-hydroxyquinoline and its coordination compound with lanthanum showed the following (see Tables 5 and 6).

Table 5. Analysis of the biological activity profile of 8-hydroxyquinoline

P_a	Activity
0.920	Glycosylphosphatidylinositol phospholipase D inhibitor
0.917	Anti-seborrheic effect
0.910	Carboxypeptidase inhibitor
0.910	Pullulanase inhibitor

Indeed, 8-hydroxyquinoline is a chelating agent. The main mechanism of antibacterial activity of this molecule is the binding of metals as a part of the active center of vital enzymes of microorganisms. Thus, carboxypeptidases (P_a=0.910), lysostaphin (P_a=0.884), and pullulanase (P_a=0.910) show an antibacterial effect by destroying proteins or carbohydrates in the cell. At the same time, glycosylphosphatidylinositol phospholipase D (GPI-PLD; P_a=0.920) cleaves the anchors to hold proteins to the membrane. 8-hydroxyquinoline also has anti-seborrheic activity (P_a=0.917), affecting the function of the sebaceous glands.

When 8-hydroxyquinoline binds to lanthanum, the molecule is stabilised due to the structural changes discussed earlier. The profile of biological activity shifts towards antioxidant defense enzymes (P_a = 0.948 – glutathione thiolesterase, P_a=0.920 – monodehydroascorbate reductase), and signaling proteins, including nicotinic and acetylcholine receptors (P_a=0.900). It indicates a decrease in redox activity and shows more selective interactions of the compound with protein targets while maintaining the antimicrobial properties of the parent ligand.

Table 6. Analysis of the biological activity profile of the La(III) complex with 8-hydroxyquinoline

P_a	Activity
0.948	Glutathione thiolesterase inhibitor
0.932	Glycosylphosphatidylinositol phospholipase D inhibitor
0.920	Carboxypeptidase inhibitor
0.920	Monodehydroascorbate reductase (NADH) inhibitor
0.907	Pullulanase inhibitor
0.900	Antagonist of nicotinic and acetylcholine receptors (α6β3β4α5)

Using program [27], we investigated the dependence of the distribution coefficient in the octanol-water system (log P) on pH for the lanthanum complex with 8-hydroxyquinoline and for the initial ligand (see Fig. 8). Analysis of the function graphs showed higher bioavailability of the coordination compound in an alkaline environment (pH=9-15) compared to the initial substance.

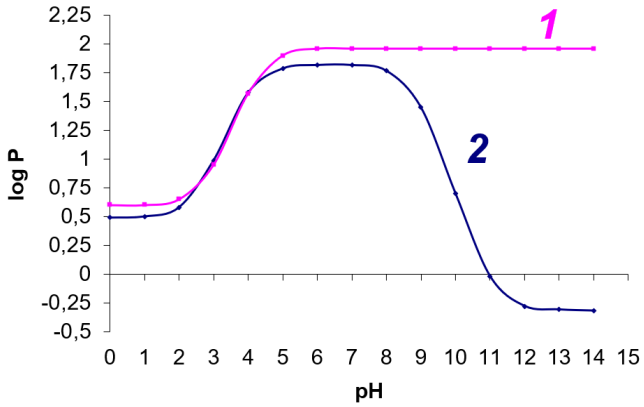

Fig. 8. The graph of log P dependence on pH for the ligand (curve 2) and the complex compound (curve 1).

Using the Swiss ADME service [28], we tested the research objects for bioavailability based on a number of formal criteria [29-30]. These criteria allow us to evaluate adsorption and assess the potential of a drug based on a number of parameters, including pharmacokinetic ones (see Table 7). Both the ligand and the complex are capable of penetrating the blood-brain barrier (BBB), adsorbed in the gastrointestinal tract, and comply with Lipinski's, Weber's, and Ethan's rules. Abbott's bioavailability index has a value of 0.55; it is the same for both compounds [31], further confirming compliance with Lipinski's rules. The La(III) complex with 8-hydroxyquinoline penetrates the skin 0.76 cm/s faster than the original ligand.

Table 7. Analysis of the biological activity profile of the La(III) complex with 8-hydroxyquinoline

Parameter	Parameter value for 8-hydroxyquinoline	The value of the parameter for the La(III) complex with 8-hydroxyquinoline
Molecular weight	145.16 g/mol	283.06 g/mol
Gastrointestinal absorption	High indicator	High indicator
Ability to permeate the blood-brain barrier (BBB)	+	+
Rate of penetration through the skin	5.75 cm/s	6.51 cm/s
Compliance with Lipinski's rule	+	+
Gouze filter	-	-
Weber filter	+	+
Egan filter	+	+
Müegge filter	-	+
Abbott bioavailability index	0.55	0.55

Conclusions

A La(III) complex with 8-hydroxyquinoline was synthesised. Analysis of IR spectra and quantum chemical calculations (MOPAC 2016 // PM7) confirmed the coordination of the metal with the ligand via the phenolic oxygen and nitrogen of the quinoline ring. The absorption maximum of the resulting coordination compound in the electronic spectrum was λ_{max}=379 nm, wave numbers in the IR spectrum: ν(C-O)=1233.8 cm^{-1}, ν(C=C)=1600.5 cm^{-1}, ν(Ar)=1569.0 cm^{-1}, ν(La^{3+}-O, La^{3+}-N)=657.0. Additionally, the participation of heteroatoms in coordination was confirmed by a change in charge during complex formation: Δq_N=0.453; Δq_O=0.426. The energy gap was ΔE_{total}= 1.5855 eV. A study of the dependence of absorption on pH showed that the complex is most stable in a neutral environment (pH = 7.0–8.0). This is consistent with its chelate nature and resistance to hydrolysis and protonation. Moreover, La(III) complex with 8-hydroxyquinoline is a more selective and potentially less toxic analogue of the original ligand, retaining the useful biochemical properties and possessing improved physiological parameters. This makes it promising for further biomedical research.

Conflict of interest

The authors declare no conflict of interest in financial or any other sphere.

References

1. **Bhagwat A., Butts A., Greve E., Cheung Y., Melief E., Gomez J., Hung D.T., Parish T.** 8-Hydroxyquinoline series exerts bactericidal activity against Mycobacterium tuberculosis via copper-mediated toxicity. *ACS Infect. Dis.* 2024, 10(**10**), 3692–3698. DOI: 10.1021/acsinfecdis.4c00582.
2. **Cipurković A., Horozić E., Marić S., Mekić L., Junuzović H.** Metal Complexes with 8-Hydroxyquinoline: Synthesis and In Vitro Antimicrobial Activity. *Open J. Appl. Sci.* 2021, 11, 1–10. DOI: 10.4236/ojapps.2021.111001.
3. **Elshahed M.S., Toubar S.S., Ashour A.A., El-Eryan R.T.** Novel sensing probe using Terbium-sensitized luminescence and 8-hydroxyquinoline for determination of prucalopride succinate: green assessment with Complex-GAPI and analytical Eco-Scale. *BMC Chem.* 2022, 16(**1**), 80. DOI: https://doi.org/10.1186/s13065-022-00876-0
4. **Avetisov R., Kazmina K., Barkanov A.** One-Step Synthesis of High-Pure Tris(8-hydroxyquinoline)aluminum for Optics and Photonics. *Materials*. 2022, 15, 734. DOI: 10.3390/ma15030734
5. **Ribeiro N., Bulut I., Ugone V., Ferreira L.P.** Promising anticancer agents based on 8-hydroxyquinoline: coordination to metal ions fosters cytotoxic activity. *Front. Chem.* 2023, 11, 1106349. DOI: 10.3389/fchem.2023.1106349.
6. **Côrte-Real L., Martins M., Fontrodona X.** Cu(II) and Zn(II) Complexes of New 8-Hydroxyquinoline Schiff Bases: Structure, Speciation, and Anticancer Potential. *Molecules* 2023, 28, 7894. DOI: 10.3390/molecules28107894.
7. **Lopes J., Romero I., Correia I., Gaspar M.M.** Novel 8-Hydroxyquinoline-Derived V(IV)O, Ni(II), and Fe(III) Complexes: Synthesis, Characterization, and Cytotoxicity. *Inorganics* 2025, 13, 150. DOI: 10.3390/2304-6740/13/5/150.
8. **Wu D.-F., Liu Z., Ren P., Liu X.-H., Wang N., Cui J.-Z., Gao H.-L.** A new family of dinuclear lanthanide complexes constructed from an 8-hydroxyquinoline Schiff base and β-diketone: magnetic properties and near-infrared luminescence. *Dalton Trans.* 2019, 48, 1392-1403. DOI: 10.1039/C8DT04384A.
9. **Saadeh H.A., Sweidan K.A., Mubarak M.S.** Recent Advances in the Synthesis and Biological Activity of 8-Hydroxyquinolines. *Molecules* 2020, 25(**18**), 4321. DOI: 10.3390/molecules25184321.
10. **Ramenskaya, L. M., Vladimirova, T. V.** The stability and solubility of cadmium (II)-8-oxyquinoline complexes in water and micellar solutions of sodium dodecyl sulfate. *Russ. J. Phys. Chem.,* 2006, 80(**6**), 904-908. DOI: https://doi.org/10.1134/S0036024406060112.
11. **Chupakhina, T. A., Katsev, A. M., Kuryanov, V. O.** Synthesis and investigation of antimicrobial activity of 8-Hydroxyquinoline glucosaminides. *Russian J. of Bioorg. Chem*. 2012, 38(**4**), 422-427. DOI: https://doi.org/10.1134/S106816201204005X
12. **Ninh, N. H., Sang, D. X. N., Hieu, D. M., Chi, N. T. T.** Anti-microbial activity of some Pt (II) complexes bearing 8-oxyquinoline (8-OQ) and eugenol derivative and 3D-structure of complex [PtCl (8-OQ)(Eugenol)]. *J. Nat. Sci.*, 2024, 118-124. DOI: https://doi.org/10.18173/2354-1059.2024-0026
13. **Al-Farhan B.S., Basha M.T., Abdalla E.M.** Synthesis, DFT Calculations, Antiproliferative, Bactericidal and Antioxidant Activities of Mixed-Ligand Metal Complexes Containing 8-Hydroxyquinoline. *Molecules* 2021, 26(**16**), 4725. DOI: 10.3390/molecules26164725.
14. **Yu, W. Y., Zhang, L. G., Qiu, J. B., Wang, J. X., Chen, C. J., Zhou, M. G.** Effect of carbendazim-8-oxyquinoline-copper, a novel chelate fungicide against Fusarium graminearum. *J. of Pest. Sci*., 2011, 36(**3**), 385-391.
15. **Yabrir B., Belhassan A., Laklifi T., Moran S. G., Buakhrin M., Kandiya G. L.** Determination inhibitors of the main protease of SARS-CoV-2 in trace amounts of components of Algerian herbal medicines using in silico methods. *Pharmacy and pharmacology.* 2025, 13 (**1**), 56-66. DOI: 10.19163/2307-9266-2025-13-1-56-66
16. **Zhang L., Shi H., Jiang Z.** Ten-Gram-Scale Mechanochemical Synthesis of Ternary Lanthanum Coordination Polymers for Antibacterial and Antitumor Activities. *Front. Chem.* 2022, 10:898324. DOI: 10.3389/fchem.2022.898324.
17. **Zhou X.** Insights of metal 8-hydroxylquinolinol complexes as the potential anticancer drugs. *J. Inorg. Biochem.* 2023, 238, 112051. DOI: 10.1016/j.jinorgbio.2022.112051.

18. **Gallo E.** Aluminium 8-Hydroxyquinolinate N-Oxide as a Precursor to Heterometallic Complexes: Synthesis and Characterization. *Molecules*. 2024, 29(**2**), 451. DOI: 10.3390/molecules29020451.
19. **He J., Zhou T., Cao Y., Zhang Y., Yang W., Ma M.** Study on relationship between fluorescence properties and structure of substituted 8-hydroxyquinoline zinc complexes. *J. Fluorescence* 2018. DOI: 10.1007/s10895-018-2275-7.
20. General Pharmacopoeia Article .1.2.1.0005.15 Solubility. The State Pharmacopoeia of the Russian Federation [Electronic resource]. Available at: https://pharmacopoeia.regmed.ru/ (accessed: 22.11.2025)
21. **Schollenberger C. J.** Ammonium acetate as a neutral buffered standard. *J. Am. Chem. Soc.* 1932, 54(**6**), 2568-2573. DOI: https://doi.org/10.1021/ja01345a515.
22. **Mandal, P., Kretzschmar, J., Drobot, B.** Not just a background: pH buffers do interact with lanthanide ions—a Europium (III) case study. *JBIC J. of Biol. Inorg. Chem.* 2022. 27(**2**), 249-260. DOI: https://doi.org/10.1007/s00775-022-01930-x
23. **Kothawade, S., Shende, P.** Coordination bonded stimuli-responsive drug delivery system of chemical actives with metal in pharmaceutical applications. *Coord. Chem. Rev*. 2024, 510, 215851. DOI: https://doi.org/10.1016/j.ccr.2024.215851.
24. **James J. P. Stewart**, MOPAC2016, Stewart Computational Chemistry, Colorado Springs, CO, USA. Available at: http://openmopac.net/ (accessed: 22.11.2025)
25. **Zhurko G.A., Zhurko D.A.** ChemCraft version 1.6 (build 312). Available at: http://www.chemcraftprog.com/index.html (accessed: 22.11.2025)
26. **Filimonov D.A., Lagunin A.A., Gloriozova T.A., Rudik A.V., Druzhilovskii D.S., Pogodin P.V., Poroikov V.V.** Prediction of the biological activity spectra of organic compounds using the PASS online web resource. *Chemistry of Heterocyclic Compounds.* 2014, 50(**3**), 444-457. DOI: https://doi.org/10.1007/s10593-014-1496-1
27. **ChemAxon** Log D vs. pH Predictor. ChemAxon. Available at: https://chemaxon.com/products/logd-predictor (accessed: 22.11.2025).
28. **Daina A., Michielin O., Zoete V.** SwissADME: a free web tool to evaluate pharmacokinetics, drug-likeness and medicinal chemistry friendliness of small molecules. *Sci. Rep*. 2017, 7, 12717. DOI: https://doi.org/10.1038/srep42717
29. **Odhiambo, D. O., Omosa, L. K., Njagi, E. C., Kithure, J. G., Wekesa, E. N.** In-silico Pharmacokinetics ADME/Tox Analysis of phytochemicals from genus Dracaena for their therapeutic potential. *Sci. Afr.* 2025, e02796. DOI: https://doi.org/10.1016/j.sciaf.2025.e02796
30. **Yadav, M., Yadav, P., Yadav, J. P., & Kataria, S. K.** Novel derivatives of Costus igneus towards potentiality against diabetes mellitus receptors: ADME/Tox profiling, Computational Docking, and Molecular Dynamics Simulation study. *J. of Taibah Univ. for Sci.* 2024, 18(**1**), 2370107. DOI: https://doi.org/10.1080/16583655.2024.2370107.
31. **Ahmad, I., Dogra, A., Nagpal, T., Sharma, C., Singh, S., Shaiva, N., Luhach, K.** Liposome-like encapsulation of fish oil-based self-nano emulsifying formulation for improved bioavailability. *Appl. Food Res.,* 2025, 5(**1**), 100745. DOI: https://doi.org/10.1016/j.afres.2025.100745.

Received 24.11.2025
Approved after reviewing 29.12.2025
Accepted 13.01.2026